Original Research Paper

Volume-9 | Issue-5 | May-2019 | PRINT ISSN No 2249 - 555X

Mathematics

HEAT AND MASS TRANSFER EFFECTS ON UNSTEADY MHD CASSON FLUID PAST A VERTICAL PLATE IN THE PRESENCE OF POROUS MEDIUM

S Veera Reddy	Department of Mathematics, Rayalaseema University, Kurnool, A.P, India
G. S. S. Raju*	Department of Mathematics, JNT University, Pulivendula, Kadapa, A.P, India *Corresponding Author
A.G. Vijaya Kumar	Department of Mathematics, SAS, VIT University, TN, India

ABSTRACT Heat and mass transfer outcomes on erratic MHD Casson fluid fluid past a vertical plate in omnipresence of Porous Medium with fluctuating temperatures and wavering concentration under the impact of uniform transverse magnetic field is investigated. The undimensional governing partial differential equations are approached with the standard integral transform technique that is unconfined. Numerical solution based graphical outcomes for the velocity distribution, temperature distribution and concentration distribution are exhibited and impact of various parameters on the skin-friction coefficent, the rate of heat transfer at the plate and the rate of mass transfer at the surface are conferred.

KEYWORDS : Casson fluid, Soret effect,magnetic field, radiation,heat and mass transfer and porous medium

INTRODUCTION:

Numerous uses for the magnetohydrodaynamics(MHD) flows of non-Newtonian fluid in a permeable medium are confronted in the optimalization of solidifying techniques of metals, biological systems, irrigation issues, paper, heat- storagebeds, metal alloys, process of petroleum, textile, geothermal surfaces scrutiny, polymer composite industries, custard, tooth paste, paints, shampoo, strach suspensions and nuclear fuel deris treatment. Countless studies have been demonsrated on several features of magnetohydrodaynamics flows of non-Newtonian fluid running through a porous medium. In certain cases no flow occurs with little shear stress implying that these particular non-Newtonian fluids function as elastic solid. One example of this is a Casson fluid. It exhibits distinct charecterstics and is highly noted in recent times. The outcomes of thermophoresis and few thermo-physical characterstics on free convective heat and mass transfer of non Darcian MHD flow past a vertical poriferous plate with nth order of chemical reaction in the existence of suction, plastic dynamic viscosity of the non- Newtonian fluid collectively with thermal conductivity investigated by Animasaun[3] are supposed to deviate as a linear function of temperature. Casson fluid flow, accompanying chemical reaction in a transverse magnetic field, over a vertical porous surface was nume studied by Emmanuel et al. [8] in a numerical approach. Hari et al. [10] examined radiation and response of chemical reaction on magnetohydrodynamic Casson fluid flowing onto an oscillating vertical plate implanted in porous medium. Hayat et al. [12] amalgamated convection stagnation point flow of Casson fluid and convective boundary constraints by employing homotopy analysis approach. Khalid et al. [14] procured an analytical explication for a wavering MHD free convection flow of Casson fluid past over an oscillating vertical plate enclosed in a permeable medium. Mabood et al. [15] determined multiple slips effects on MHD Casson fluid flow in porous medium alongwith radiation and chemical reaction. Pramanik [20] analysed numerical outcomes for steady boundary layer flow and heat transfer for a Casson fluid over an exponentially permeable stretching surface along with existence of thermal radiation. Shehzad et al. [23] determined the outcomes of mass transfer on the MHD boundary layer flow of a Casson fluid model alongwith chemical reaction. Charactertics for non-Newtonian fluid flow and heat transfer over a nonlinearly stretching surface were depicted by Swati [25]. The Casson fluid standard model is employed to potray the non- Newtonian fluid behavior.

The compound heat and mass transfer problems combined along with chemical reactions are significant to various processes, hence have received a high recognition currently in recent years. In treatments and processes such as drying, evaporation at the surface of a water body, energy transfer in a wet cooling tower and the flow in a desert cooler, concomitant heat and mass transfer takes place. Chemical reactions can be codified as likewise homogeneous course of action. A homogeneous reaction eventuates steadily though a throughout a given phase, while a heterogeneous reaction happens in a confined region or within the phase edge. A first order reaction is in which the rate of reaction is directly proportional to the concentration itself. A chemical reaction of a foreign mass and the fluid takes place in various chemical engineering processes and treatments. These processes are encountered in several industrial applications, like the polymer production, the production of ceramics or glassware, the food processing etc. Alam and Rahman [1] examined the Dufour and Soret effects on MHD free convective heat and mass transfer flow over a vertical porous flat plate implanted in porous medium. Ahmmed [2] procured analytical solution for the fluctuating MHD free convection and mass transfer flowing onto a vertical permeable plate. Chamaka et al. [4] determined the hydromagnetic combined heat and mass transfer by natural convection from a permeable surface introduced in a fluid saturated porous medium. Outcomes of mass transfer on flow over an impulsively started infinite vertical plate with steady heat flux along with a chemical reaction was studied by Das et al. [7]. Hayat et al. [11] has depicted heat and mass transfer for Soret and Dufour effects on amalgamated convection boundary layer flow over a stretching vertical surface in a porous medium full of a a viscoelastic fluid. Hassain et al. [13] have determined the results of radiation on the natural convection flow of an optically dense incompressible fluid along with a evenly heated vertical plate with a constant suction. Makinde [16] studied MHD boundary layer flow and mass transfer past a vertical plate in a porous medium with unwavering heat flux. Makinde[16] and Aziz [17] depicted the MHD mixed convection from a vertical plate introduced in a porous medium with a convective boundary restrictions . Magnetohydrodynamics (MHD) and radiation impact on a moving isothermal vertical plate with inconstant and mass diffusion is investigated by Muthucumaraswamy and Janakiraman [19]. The results of heat generation or absorption on hydromagnetic boundary layer flow of a vertical flat plate in motion, embedded with suction, is depicted by Rushi Kumar and Gangadhar [21]. Rushi Kumar et al. [22] procured exact resolution of Soret and radiation effects on inconstant natural convection flow in the existence of magnetic field fixed in relation to the Fluid or to the Plate. Soundalgekar et al. [24] studied on the MHD Stokes problem for a vertical plate with changing temperature. Accurate resolution of the wavering magneto hydrodynamic free convection flows was analysed by Tokis [26].

From bibliography , it can be inferred that not much significant attention is given over the heat and mass transfer effects and analysis on unsteady MHD Casson fluid fluid passing over a vertical plate in the presence of Porous Medium with variable temperature and mass diffusion under the influence of uniform transvers magnetic field although this situation takes in manifold engineering applications. Integral transform technique is applied to rule out non-dimensional governing equations.

Mathematical Analysis:

Taking into account the heat and mass transfer results on inconstant

MHD Casson fluid fluid past a vertical plate in the presence of Porous Medium with changing temperature and wavering concentration under the influence of uniform transvers magnetic field. The x'-axis is taken along the vertical plate in the upward direction, and y' - axis is normal to it.A uniform magnetic field of strength $0B$ is applied perpendicular to the fluid flow direction. Initially it is assumed that at time0,t'≤both the plate and surrounding fluid are at the same temperature and concentration in stationary condition for all the points in entire flow region0y'≥. At time 0,t'>the plate starts moving with exponential velocity 0exp()$uuat''$=in x'- direction. Concurrently, the plate temperature is inflated linearly with time t and also the mass is diffused from the plate linearly with time. The fluid is supposed to emit gray and absorb radiation but in non- scattering medium. It's also considered that the applied magnetic field is steady and that the magnetic Reynolds number is small so that the induced magnetic field is overlooked. All the fluid properties are assumed to be persistent excluding the persuation of the density variation with temperature in the body force term. Electric field and dissipation outcomes are ignored. The constitutive equation for the Casson fluid can be written as (Mustafa eat al. [18])

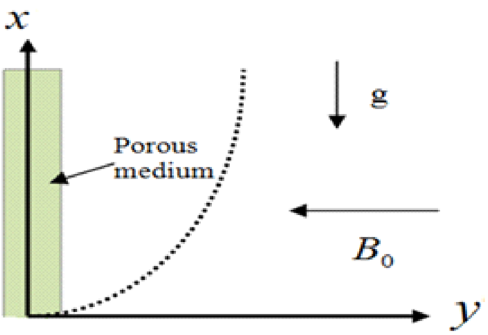

Fig. 1 Physical co-ordinate system

$$\tau_{ij} = \begin{cases} 2\left(\mu_B + \dfrac{P_y}{\sqrt{2\pi}}\right) e_{ij} & \pi > \pi_c\ , \\ 2\left(\mu_B + \dfrac{P_y}{\sqrt{2\pi_c}}\right) e_{ij} & \pi < \pi_c \end{cases}$$

Where $\pi_j = e_{ij} e_{ij}$ and $ij e$is the (i, j)th component of the rate of deformation, π is the product of the component of rate of deformation with itself, π_c is a critical value of this product which is based on the non-Newtonian model, P_y is yield stress of fluid and μ_B is plastic dynamic viscosity of the non-Newtonian fluid. According to these assumptions, the equations describing the physical situation are given by

$$\frac{\partial u'}{\partial t'} = \nu\left(1+\frac{1}{\gamma}\right)\frac{\partial^2 u'}{\partial y'^2} + g\beta(T'-T'_\infty) + g\beta^*(C'-C'_\infty) - \frac{\sigma B_0^2 u'}{\rho} - \nu\frac{u'}{K'} \tag{1}$$

$$\rho c_p \frac{\partial T'}{\partial t'} = k\frac{\partial^2 T'}{\partial y'^2} - \frac{\partial q_r}{\partial y'} + Q'(T'_\infty - T') \tag{2}$$

$$\frac{\partial C'}{\partial t'} = D\frac{\partial^2 C'}{\partial y'^2} + D_1\frac{\partial^2 T'}{\partial y'^2} - k'(C'-C'_\infty) \tag{3}$$

With the following initial and boundary conditions

$$t' \le 0 : u' = 0,\ T' = T'_\infty\ \ C' = C'_\infty,\ \ \text{for all } y'$$
$$t' > 0 : u' = u_0 \exp(a't')\ T' = T'_\infty + (T'_w - T'_\infty) A t'$$
$$C' = C'_\infty + (C'_w - C'_\infty) A t' \quad \text{at } y' = 0$$
$$u' = 0,\ T' \to T'_\infty,\ C' \to C'_\infty,\ \text{as } y' \to \infty \tag{4}$$

Where $A = \dfrac{u_0^2}{\nu}$ the local radiant for the case of an optically thin gray gas is expressed by (Cogly et al. [5])

$$\frac{\partial q_r}{\partial y'} = -4a^*\sigma\left(T'^4_\infty - T'^4\right) \tag{5}$$

Assumption is made that the temperature variations within the flow are small enough and that T'^4may be expressed as a linear function of the temperature. This is obtained by expanding T'^4 in a Taylor series about $T\infty'$ and the higher order terms neglected, So we get

$$T^4 \cong T_\infty^4 + 4TT_\infty^3 - 4T_\infty^4$$
$$T'^4 \cong 4T'^3_\infty T' - 3T'^4_\infty$$
$$T'^4 \cong T_\infty^4 + 4T_\infty^3(T - T_\infty) \tag{6}$$

From Esq. (5) and (6), Eq. (2) reduces to

$$\rho c_p \frac{\partial T'}{\partial t'} = k\frac{\partial^2 T'}{\partial t'^2} + 16a^*\sigma T'^3_\infty (T'_\infty - T') \tag{7}$$

On introducing the following non- dimensional quantities

$$u = \frac{u'}{u_0},\ t = \frac{t'u_0^2}{\nu},\ y = \frac{y'u_0}{\nu},\ \theta = \frac{T'-T'_\infty}{T'_w - T'_\infty},\ C = \frac{C'-C'_\infty}{C'_w - C'_\infty},\ Gr = \frac{g\beta\nu(T'_w - T'_\infty)}{u_0^3},\ Gm = \frac{g\beta^*\nu(C'_w - C'_\infty)}{u_0^3},$$
$$\Pr = \frac{\mu C_p}{k},\ Sc = \frac{\nu}{D},\ S_0 = \frac{D_1(T'_w - T'_\infty)}{\nu(C'_w - C'_\infty)},\ M = \frac{\sigma B_0^2 \nu}{\rho u_0^2},\ R = \frac{16a^*\nu^2\sigma T'^3_\infty}{k u_0^2},\ a_0 = \frac{a'\nu}{u_0^2},\ H = \frac{Q'\nu^2}{k u_0^2},\ k = \frac{\nu k'}{u_0^2},\ K = \frac{K'u_0^2}{\nu^2}, \tag{8}$$

We get the following governing equations which are dimensionless.

$$\frac{\partial u}{\partial t} = \left(1+\frac{1}{\gamma}\right)\frac{\partial^2 u}{\partial y^2} + Gr\theta + GmC - \left(M + \frac{1}{K}\right)u \tag{9}$$

$$\frac{\partial \theta}{\partial t} = \frac{1}{\Pr}\frac{\partial^2 \theta}{\partial y^2} - \frac{1}{\Pr}(R + H)\theta \tag{10}$$

$$\frac{\partial C}{\partial t} = \frac{1}{Sc}\frac{\partial^2 C}{\partial y^2} + S_0\frac{\partial^2 \theta}{\partial y^2} - kC \tag{11}$$

The initial and boundary conditions in dimensionless form are as follows:

$$t \le 0 : u = 0,\quad \theta = 0,\quad C = 0 \qquad \text{for all } y,$$
$$t > 0 : u = e^{a_0 t},\ \theta = t,\quad C = t \qquad \text{at } y = 0,$$
$$u \to 0,\ \theta \to 0,\quad C \to 0 \quad as \quad y \to \infty \tag{12}$$

The physical parameters appeared are defined in the nomenclature. Laplace transform technique is used to solve the dimensionless governing equations form (9) to (11), subject to the boundary conditions (12) and the solutions are conveyed in terms of complementary and exponential error functions.

$$\theta(y,t) = \left[\left(\frac{t}{2} + \frac{y\Pr}{4\sqrt{A}}\right)\exp\left(y\sqrt{A}\right)erfc\left(\frac{y\sqrt{\Pr}}{2\sqrt{t}} + \sqrt{\frac{At}{\Pr}}\right) + \left(\frac{t}{2} - \frac{y\Pr}{4\sqrt{A}}\right)\exp\left(-y\sqrt{A}\right)erfc\left(\frac{y\sqrt{\Pr}}{2\sqrt{t}} - \sqrt{\frac{At}{\Pr}}\right)\right] \tag{13}$$

$$\begin{aligned} C(y,t) = {} & a_7\left[\left(\frac{t}{2} + \frac{y\sqrt{Sc}}{4\sqrt{k}}\right)\exp\left(y\sqrt{kSc}\right)erfc\left(\frac{y\sqrt{Sc}}{2\sqrt{t}} + \sqrt{kt}\right) + \left(\frac{t}{2} - \frac{y\sqrt{Sc}}{4\sqrt{k}}\right)\exp\left(-y\sqrt{kSc}\right)erfc\left(\frac{y\sqrt{Sc}}{2\sqrt{t}} - \sqrt{kt}\right)\right] \\ & + \frac{(a_4 - a_6)}{2}\left[\exp\left(y\sqrt{kSc}\right)erfc\left(\frac{y\sqrt{Sc}}{2\sqrt{t}} + \sqrt{kt}\right) + \exp\left(-y\sqrt{kSc}\right)erfc\left(\frac{y\sqrt{Sc}}{2\sqrt{t}} - \sqrt{kt}\right)\right] \\ & + \frac{(-a_4 + a_6)}{2}\exp(-a_2 t)\left[\exp\left(y\sqrt{(k-a_2)Sc}\right)erfc\left(\frac{y\sqrt{Sc}}{2\sqrt{t}} + \sqrt{(k-a_2)t}\right) + \exp\left(-y\sqrt{(k-a_2)Sc}\right)erfc\left(\frac{y\sqrt{Sc}}{2\sqrt{t}} - \sqrt{(k-a_2)t}\right)\right] \\ & + a_5\left[\left(\frac{t}{2} + \frac{y\Pr}{4\sqrt{A}}\right)\exp\left(y\sqrt{A}\right)erfc\left(\frac{y\sqrt{\Pr}}{2\sqrt{t}} + \sqrt{\frac{At}{\Pr}}\right) + \left(\frac{t}{2} - \frac{y\Pr}{4\sqrt{A}}\right)\exp\left(-y\sqrt{A}\right)erfc\left(\frac{y\sqrt{\Pr}}{2\sqrt{t}} - \sqrt{\frac{At}{\Pr}}\right)\right] \\ & + \frac{(-a_4 + a_6)}{2}\left[\exp\left(y\sqrt{A}\right)erfc\left(\frac{y\sqrt{\Pr}}{2\sqrt{t}} + \sqrt{\frac{At}{\Pr}}\right) + \exp\left(-y\sqrt{A}\right)erfc\left(\frac{y\sqrt{\Pr}}{2\sqrt{t}} - \sqrt{\frac{At}{\Pr}}\right)\right] \\ & + \frac{(a_4 - a_6)}{2}\exp(-a_2 t)\left[\exp\left(y\sqrt{A - a_2\Pr}\right)erfc\left(\frac{y\sqrt{\Pr}}{2\sqrt{t}} + \sqrt{\frac{At}{\Pr} - a_2 t}\right) + \exp\left(-y\sqrt{A - a_2\Pr}\right)erfc\left(\frac{y\sqrt{\Pr}}{2\sqrt{t}} - \sqrt{\frac{At}{\Pr} - a_2 t}\right)\right] \end{aligned} \tag{14}$$

$$u(y,t) = \frac{\exp(a_0 t)}{2}\left[\exp\left(y\sqrt{b_4}\right)erfc\left(\frac{y}{2\sqrt{Bt}} + \sqrt{b_4 t}\right) + \exp\left(-y\sqrt{b_4}\right)erfc\left(\frac{y}{2\sqrt{Bt}} - \sqrt{b_4 t}\right)\right]$$

$$
\begin{aligned}
&+\frac{A_0}{2}\left[\exp\left(y\sqrt{b}\right)erfc\left(\frac{y}{2\sqrt{Bt}}+\sqrt{bt}\right)+\exp\left(-y\sqrt{b}\right)erfc\left(\frac{y}{2\sqrt{Bt}}-\sqrt{bt}\right)\right]\\
&+\frac{A_1}{2B}\left[\left(\frac{t}{2}+\frac{y}{4\sqrt{b}}\right)\exp\left(y\sqrt{b}\right)erfc\left(\frac{y}{2\sqrt{Bt}}+\sqrt{bt}\right)+\left(\frac{t}{2}-\frac{y}{4\sqrt{b}}\right)\exp\left(-y\sqrt{b}\right)erfc\left(\frac{y}{2\sqrt{Bt}}-\sqrt{bt}\right)\right]\\
&+\frac{A_2\exp(-a_8t)}{2}\left[\exp\left(y\sqrt{b_1}\right)erfc\left(\frac{y}{2\sqrt{Bt}}+\sqrt{b_1t}\right)+\exp\left(-y\sqrt{b_1}\right)erfc\left(\frac{y}{2\sqrt{t}}-\sqrt{b_1t}\right)\right]\\
&+\frac{A_3\exp(-a_{10}t)}{2}\left[\exp\left(y\sqrt{b_2}\right)erfc\left(\frac{y}{2\sqrt{Bt}}+\sqrt{b_2t}\right)+\exp\left(-y\sqrt{b_2}\right)erfc\left(\frac{y}{2\sqrt{t}}-\sqrt{b_2t}\right)\right]\\
&+\frac{A_4\exp(-a_2t)}{2}\left[\exp\left(y\sqrt{b_3}\right)erfc\left(\frac{y}{2\sqrt{Bt}}+\sqrt{b_3t}\right)+\exp\left(-y\sqrt{b_3}\right)erfc\left(\frac{y}{2\sqrt{t}}-\sqrt{b_3t}\right)\right]\\
&+\frac{A_5}{2}\left[\exp\left(y\sqrt{A}\right)erfc\left(\frac{y\sqrt{\Pr}}{2\sqrt{t}}+\sqrt{\frac{At}{\Pr}}\right)+\exp\left(-y\sqrt{A}\right)erfc\left(\frac{y\sqrt{\Pr}}{2\sqrt{t}}-\sqrt{\frac{At}{\Pr}}\right)\right]\\
&+A_6\left[\left(\frac{t}{2}+\frac{y\Pr}{4\sqrt{A}}\right)\exp\left(y\sqrt{A}\right)erfc\left(\frac{y\sqrt{\Pr}}{2\sqrt{t}}+\sqrt{\frac{At}{\Pr}}\right)+\left(\frac{t}{2}-\frac{y\Pr}{4\sqrt{A}}\right)\exp\left(-y\sqrt{A}\right)erfc\left(\frac{y\sqrt{\Pr}}{2\sqrt{t}}-\sqrt{\frac{At}{\Pr}}\right)\right]\\
&+\frac{A_7\exp(-a_2t)}{2}\left[\exp\left(y\sqrt{A-a_2\Pr}\right)erfc\left(\frac{y\sqrt{\Pr}}{2\sqrt{t}}+\sqrt{\frac{At}{\Pr}-a_2t}\right)+\exp\left(-y\sqrt{A-a_2\Pr}\right)erfc\left(\frac{y\sqrt{\Pr}}{2\sqrt{t}}-\sqrt{\frac{At}{\Pr}-a_2t}\right)\right]\\
&+\frac{A_8\exp(-a_8t)}{2}\left[\exp\left(y\sqrt{A-a_8\Pr}\right)erfc\left(\frac{y\sqrt{\Pr}}{2\sqrt{t}}+\sqrt{\frac{At}{\Pr}-a_8t}\right)+\exp\left(-y\sqrt{A-a_8\Pr}\right)erfc\left(\frac{y\sqrt{\Pr}}{2\sqrt{t}}-\sqrt{\frac{At}{\Pr}-a_8t}\right)\right]\\
&+\frac{A_9}{2}\left[\exp\left(y\sqrt{kSc}\right)erfc\left(\frac{y\sqrt{Sc}}{2\sqrt{t}}+\sqrt{kt}\right)+\exp\left(-y\sqrt{kSc}\right)erfc\left(\frac{y\sqrt{Sc}}{2\sqrt{t}}-\sqrt{kt}\right)\right]\\
&+A_{10}\left[\left(\frac{t}{2}+\frac{y\sqrt{Sc}}{4\sqrt{k}}\right)\exp\left(y\sqrt{kSc}\right)erfc\left(\frac{y\sqrt{Sc}}{2\sqrt{t}}+\sqrt{kt}\right)+\left(\frac{t}{2}-\frac{y\sqrt{Sc}}{4\sqrt{k}}\right)\exp\left(-y\sqrt{kSc}\right)erfc\left(\frac{y\sqrt{Sc}}{2\sqrt{t}}-\sqrt{kt}\right)\right]\\
&+\frac{A_{11}\exp(-a_2t)}{2}\left[\exp\left(y\sqrt{(k-a_2)Sc}\right)erfc\left(\frac{y\sqrt{Sc}}{2\sqrt{t}}+\sqrt{(k-a_2)t}\right)+\exp\left(-y\sqrt{(k-a_2)Sc}\right)erfc\left(\frac{y\sqrt{Sc}}{2\sqrt{t}}-\sqrt{(k-a_2)t}\right)\right]\\
&+\frac{A_{12}\exp(-a_{10}t)}{2}\left[\exp\left(y\sqrt{(k-a_{10})Sc}\right)erfc\left(\frac{y\sqrt{Sc}}{2\sqrt{t}}+\sqrt{(k-a_{10})t}\right)+\exp\left(-y\sqrt{(k-a_{10})Sc}\right)erfc\left(\frac{y\sqrt{Sc}}{2\sqrt{t}}-\sqrt{(k-a_{10})t}\right)\right]
\end{aligned}
\tag{15}
$$

Where

$$A=R+H,\ B=\left(1+\frac{1}{\gamma}\right),\ b=\frac{N}{B},\ b_1=\frac{(N+a_8)}{B},\ b_2=\frac{(N+a_{10})}{B},\ b_3=\frac{(N+a_1)}{B},\ b_4=\frac{(N-a_0)}{B}$$

$$N=M+\frac{1}{K}\ a_1=\frac{-Sc\,S_oA}{(\Pr-Sc)},\ a_2=\frac{A-kSc}{(\Pr-Sc)}\ a_3=\frac{-PrSoSc}{\Pr-Sc},\ a_4=\frac{a_1}{a_2^2},\ a_5=\frac{a_1}{a_2},\ a_6=\frac{a_3}{a_2},\ a_7=\frac{-GrB}{\Pr B-1},$$

$$a_8=\frac{AB-N}{\Pr B-1},\ a_9=\frac{GmB}{BSc-1},\ a_{10}=\frac{kBSc-N}{BSc-1},\ a_{11}=\frac{GmB}{B\Pr-1},\ a_{12}=\frac{a_7}{Ba_8^2},\ a_{13}=\frac{a_7}{Ba_8},\ a_{14}=\frac{a_9}{Ba_{10}^2},\ a_{15}=\frac{a_9}{Ba_{10}},$$

$$a_{16}=\frac{a_1a_9(a_2+a_{10})}{Ba_2^2a_{10}^2},\ a_{17}=\frac{a_1a_9}{Ba_2a_{10}},\ a_{18}=\frac{a_1a_9}{Ba_{10}^2(a_2-a_{10})},\ a_{19}=\frac{a_1a_9}{Ba_2^2(a_2-a_{10})},\ a_{20}=\frac{a_3a_9}{Ba_2a_{10}},$$

$$a_{21}=\frac{a_3a_9}{Ba_{10}(a_2-a_{10})},\ a_{22}=\frac{a_3a_9}{Ba_2(a_2-a_{10})},\ a_{23}=\frac{a_1a_{11}(a_2+a_8)}{Ba_2^2a_8^2},\ a_{24}=\frac{a_1a_{11}}{Ba_2a_8},\ a_{29}=\frac{a_3a_{11}}{Ba_2(a_2-a_8)},$$

$$a_{26}=\frac{a_1a_{11}}{Ba_2^2(a_2-a_8)},\ a_{25}=\frac{a_1a_{11}}{Ba_8^2(a_2-a_8)},\ a_{27}=\frac{a_3a_{11}}{Ba_2a_8},\ a_{28}=\frac{a_3a_{11}}{Ba_8(a_2-a_8)},$$

$$A_0=(a_{12}-a_{14}+a_{16}-a_{20}-a_{23}+a_{27}),\ A_1=(-a_{13}+a_{15}-a_{17}+a_{24}),\ A_2=(-a_{12}+a_{25}-a_{28}),\ A_3=(a_{14}-a_{18}+a_{21}),$$

$$A_4=(a_{19}-a_{22}-a_{26}+a_{29}),\ A_7=(a_{26}-a_{29})\ A_5=(-a_{12}+a_{23}-a_{27}),\ A_6=(a_{13}-a_{24})\ A_9=(a_{14}-a_{16}+a_{20}),$$

$$A_8=(a_{12}-a_{25}+a_{28}),\ A_{10}=(-a_{15}+a_{17})\ A_{11}=(-a_{19}+a_{22}),\ A_{12}=(-a_{14}+a_{18}-a_{21}),$$

Skin- friction:

From velocity field, the expression for skin-friction at the plate which is given in non-dimensional forms as follows:

$$Cf=-\left[\frac{\partial u}{\partial y}\right]_{y=0} \tag{16}$$

From equations.(15) and (16), we get the expression for skin- friction at the plate as follows:

$$
\begin{aligned}
Cf=&-\exp(a_0t)\left[-\exp(-b_4t)\frac{1}{\sqrt{B\pi t}}+\sqrt{b_4}erf(\sqrt{b_4t})\right]-A_0\left[-\exp(-bt)\frac{1}{\sqrt{B\pi t}}+\sqrt{b}erf(\sqrt{bt})\right]\\
&-\frac{A_1}{B}\left[-2\exp(-bt)\sqrt{\frac{t}{B\pi}}+2t\sqrt{b}erf(\sqrt{bt})+\frac{1}{\sqrt{b}}erf(\sqrt{bt})\right]\\
&-A_2\exp(-a_8t)\left[-\exp(-b_1t)\frac{1}{\sqrt{B\pi t}}+\sqrt{b_1}erf(\sqrt{b_1t})\right]-A_3\exp(-a_{10}t)\left[-\exp(-b_2t)\frac{1}{\sqrt{B\pi t}}+\sqrt{b_2}erf(\sqrt{b_2t})\right]\\
&-A_3\exp(-a_2t)\left[-\exp(-b_3t)\frac{1}{\sqrt{B\pi t}}+\sqrt{b_3}erf(\sqrt{b_3t})\right]-A_5\left[\left(-\exp(-\frac{At}{\Pr})\right)\sqrt{\frac{\Pr}{\pi t}}+\sqrt{A}erf(\sqrt{\frac{At}{\Pr}})\right]\\
&-A_6\left[\left(-2\exp(-\frac{At}{\Pr})\right)\sqrt{\frac{\Pr t}{\pi}}+2t\sqrt{A}erf(\sqrt{\frac{At}{\Pr}})+\frac{\Pr}{\sqrt{A}}erf\left(\sqrt{\frac{At}{\Pr}}\right)\right]\\
&-A_7\exp(-a_2t)\left[\left(-\exp\left(-\frac{At}{\Pr}+a_2t\right)\right)\sqrt{\frac{\Pr}{\pi t}}+\sqrt{A-a_2\Pr}erf\left(\sqrt{\frac{At}{\Pr}-a_2t}\right)\right]\\
&-A_8\exp(-a_8t)\left[\left(-\exp\left(-\frac{At}{\Pr}+a_8t\right)\right)\sqrt{\frac{\Pr}{\pi t}}+\sqrt{A-a_8\Pr}erf\left(\sqrt{\frac{At}{\Pr}-a_8t}\right)\right]\\
&-A_9\left[\left(-\exp(-kt)\right)\sqrt{\frac{Sc}{\pi t}}+\sqrt{kSc}erf\left(\sqrt{kt}\right)\right]-A_{10}\left[-2\left(-\exp(-kt)\right)\sqrt{\frac{Sct}{\pi}}+2t\sqrt{kSc}erf\left(\sqrt{kt}\right)+\sqrt{\frac{Sc}{K}}erf(\sqrt{Kt})\right]\\
&-A_{11}\exp(-a_2t)\left[\left(-\exp\left(-kt+a_2t\right)\right)\sqrt{\frac{Sc}{\pi t}}+\sqrt{kSc-a_2Sc}erf\left(\sqrt{kt-a_2t}\right)\right]\\
&-A_{12}\exp(-a_{10}t)\left[\left(-\exp\left(-kt+a_{10}t\right)\right)\sqrt{\frac{Sc}{\pi t}}+\sqrt{kSc-a_{10}Sc}erf\left(\sqrt{kt-a_{10}t}\right)\right]
\end{aligned}
\tag{17}
$$

Nusselt Number:

From temperature field, the Nusselt number which is given in non-dimensional form as follows:

$$Nu=-\left[\frac{\partial\theta}{\partial y}\right]_{y=0} \tag{18}$$

From Eqs. (13) and (18), we get Nusselt number as follows :

$$Nu=\left[t\sqrt{A}\,erf\sqrt{\frac{At}{\Pr}}+\sqrt{\frac{t\Pr}{\pi}}\exp\left(-\frac{At}{\Pr}\right)+\frac{\Pr}{2\sqrt{A}}erf\sqrt{\frac{At}{\Pr}}\right] \tag{19}$$

Sherwood Number:

From concentration field, Sherwood Number which is given in non –dimensional form as follows

$$Sh=-\left[\frac{\partial C}{\partial y}\right]_{y=0} \tag{20}$$

From Eqs. (14) and (20) we get Sherwood Number as follows:

$$Sh=(a_5-1)\left[\exp(-kt)\sqrt{\frac{tSc}{\pi}}+t\sqrt{kSc}\,efr\left(\sqrt{kt}\right)+\frac{\sqrt{Sc}}{2\sqrt{k}}erf\left(\sqrt{kt}\right)\right]$$
$$+(a_4-a_6)\left[\exp(-kt)\sqrt{\frac{Sc}{\pi t}}-\sqrt{kSc}\,erf\left(\sqrt{kt}\right)\right]$$
$$-(-a_4+a_6)\exp(-a_2t)\left[-\exp(kt-a_2t)\sqrt{\frac{Sc}{\pi t}}+\sqrt{(k-a_2)Sc}\,erf\left(\sqrt{(k-a_2)t}\right)\right]$$
$$-a_5\left[-\exp\left(-\frac{At}{\Pr}\right)\sqrt{\frac{\Pr t}{\pi}}+t\sqrt{A}\,erf\left(\frac{At}{\Pr}\right)+\frac{\Pr}{2\sqrt{A}}erf\left(\sqrt{\frac{At}{\Pr}}\right)\right]$$
$$-(-a_4+a_6)\left[-\exp\left(-\frac{At}{\Pr}\right)\sqrt{\frac{\Pr}{\pi t}}+\sqrt{A}\,erf\left(\sqrt{\frac{At}{\Pr}}\right)\right]$$
$$-(a_4-a_6)\left[-\exp\left(-\frac{At}{\Pr}\right)\sqrt{\frac{\Pr}{\pi t}}+\exp(-a_2t)\sqrt{A-a_2\Pr}\,erf\left(\sqrt{\frac{At}{\Pr}-a_2t}\right)\right] \tag{21}$$

RESULTS AND DISCUSSIONS:

Laplace transform technique was used to solve analytically the equations (9), (10) and (11) with the boundary condition. To provide current physical insight into the problem, a set of results is reported graphically from Figs. 2- 19. These graphs were obtained from the analytical results of the numerical evaluation, desicribed in the previous section. These obtained results, reveal the effect of various physical parameters like magnetic parameter (*M*), Casson parameter (γ), heat source parameter (*H*), radiation parameter (*R*), Prandtl number (*Pr*), Schmidt parameter (*Sc*), Soret number (*So*), mass Grashof number (*Gm*) thermal Grashof number (*Gr*), on the temperature, concentration, skin- friction coefficient, the velocity, the rate of mass transfer profiles and the rate of heat transfer.

The figures (2) to (8) shows the velocity profiles of exponentially accelerated plate, when γ=0.5, *R*=2, *H*=1, *K*=1, *Sc*=2.01, *Pr* =0.71, *t*=0.4, *k*=0.5, *So*=1, *M*=5, a_o=0.5. The figures (2) to (8) shows the effects on velocity field due to *So*, *Sc, k*, *Pr*, *R*, *M*, ,γ and *H*. Fig. 2 unveils that the outcomes on fluid velocity due to effective magnetic field parameter and it shows that velocity keeps on reducing if relative to the fluid for *Pr* = 0.71 on increase in magnetic parameter. As the magnetic field parameter increases, there is decrease in the the velocity field along the surface. Close to the surface of the plate the effects are found to be stronger. This shows that the fluid velocity reduces as the magnetic field increases and the fact of forming of dragon force due to application of magnetic field on electronically conducting fluid is confirmed which results in decrease of fluid velocity. From Fig. 3 it can be noticed that increase in value of Casson parameter results in increase of velocity due to thin boundary layer thickness. This is the result of plasticity of Casson fluid. The plasticity of the fluid increases as Casson parameter decreases, which results in the increment in the velocity boundary layer thickness. Illustrations from the Fig. 4 shows with an increasing *So*, the velocity increases from which we conclude that due to greater thermal diffusion the fluid velocity increases. Fig. 5 shows, with an increasing value of *Sc* velocity increase is observed. As the Schmidt number is dependent on mass diffusion, rise in Schmidt number results in increase of mass diffusion and the velocity profile reduces. Fig. 6 unveils that with an increase in value of k, the velocity increases. Fig. 7 illustrates, the velocity decrease with increase in the values of Prandtl number. This is cause of the fact that rise in Prandtl number, fluid has lower thermal conductivity comparatively, which leads to reduction in conduction and which further reduces the thermal boundary layer thickness and due to all, velocity decreases. Fig. 8 depicts rising value of *R* or *H* or *t* results to decrease in velocity. Figs. 9 and 10. depicts the influence of various flow parameters on the fluid temperature. Fig. 9 shows that with rising values of heat source parameter, radiation parameter the fluid temperature decreses at higher rate, hence the use of radiation can used to control the temperature distribution. Fig. 10 illustrates that due to rise in values of Prandtl number, the temperature reduces. This is due to fact that an increase in Prandtl number fluid has low thermal conductivity comparatively which reduces conduction and which further results in reduction of thermal boundary layer thickness and as a result of all, temperature reduces, agrees with Hari et al.[10].

Figs. 11-14 shows the profiles of species concentration for various values of Soret effect *So,* Schmidt number *Sc*, , radiation parameter *R*, chemical reaction *k* and heat source parameter *H*. Fig.11 illustrates with the rising values of *So*, the species concentration rises. These effects are comparatively stronger on the surface closer to the plate. This depicts that as a result of greater thermal diffusion, fluid species concentration increases, agrees with Ahmmed [2] Fig. 12 unveils that the concentration due to deviation in Schmidth number for gases like ammonia (*Sc*=0.78), carban dioxide(*Sc*= 0.96) and methenol (*Sc*=1.0). It is observed that concentration field steadily dwindles for ammonia and accrues for methenol as compared to carban dioxide. Decrease in the species concentration boundary layer thickness is observed due to increase in Schmidt number. Figs. 13 depicts, as there is increase in chemical reaction parameter *k,* species concentration decreases. Figs. 14 illustrates that the result of increasing values radiation parameter is increase in fluid species concentration heat source parameter. This is result of the fact that thermal boundary layer thickness increase.

From Fig. 15 unveils the variation of Nusselt number against time *t*. Increasing values of *R* for both air and water results in increase of Nusselt number. It can also be noticed that rate of variation of heat transfer at the plate for water is more as compared to that of air. The reason is that minor values of *Pr* are equivalent to increasing the thermal conductivities and hence, heat is spread away from the plate faster than higher values of *Pr*, as the rate of heat transfer is reduced. From Figs. 16 and 17, the effects *So* and *Sc* Sherwood number against time *t* were shown. Increasing values of *So* and *Sc* results in decrease of Sherwood number. This occurs due to decrease in the fluid thermal boundary layer at the plate. Fig. 18 illustrates that with the rise of magnetic parameter, the rate of change of velocity increases. This is a result of rise of magnetic interactions at the plate. From Fig. 19 it is observed that the rate at which velocity changes is increased as the values of Soret number increases.

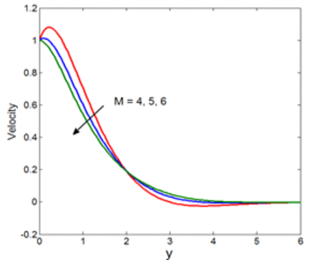

Figure 2: Transverse velocity profiles for various values of M

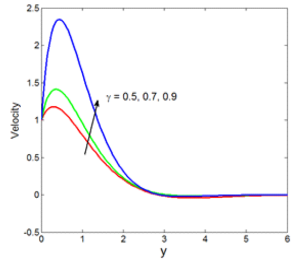

Figure 3: Transverse velocity profiles for various values of γ

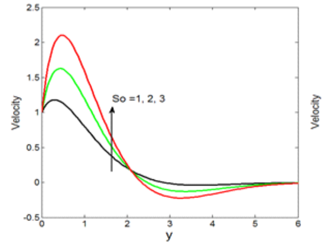

Figure 4: Transverse velocity profiles for various values of So

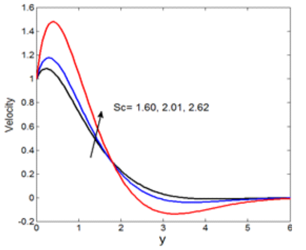

Figure 5: Transverse velocity profiles for various values of *Sc*

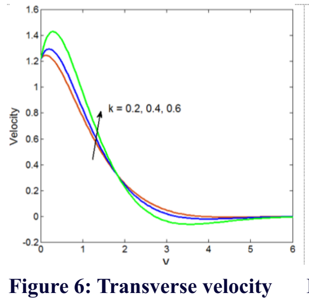

Figure 6: Transverse velocity profiles for various values of *k*

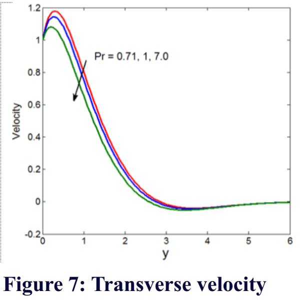

Figure 7: Transverse velocity profiles for various values of Pr

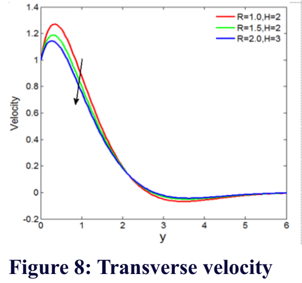

Figure 8: Transverse velocity profiles for various values of *R* and *H*

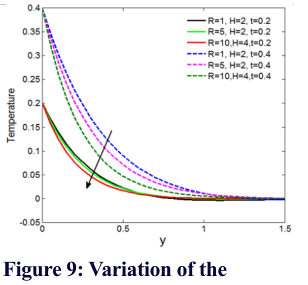

Figure 9: Variation of the temperature profiles for various values of *R, H* and *t*

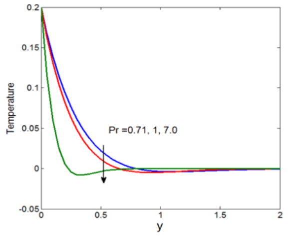

Figure 10: Variation of the temperature profiles for various values of Pr

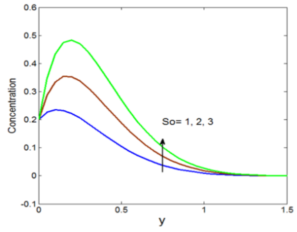

Figure 11: Species concentration profiles for various values of *So* when R=1

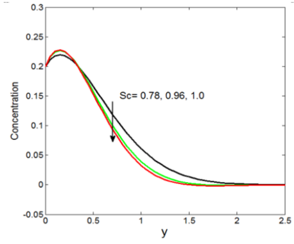

Figure 12: Species concentration profiles for various values of *Sc* when *R*=1

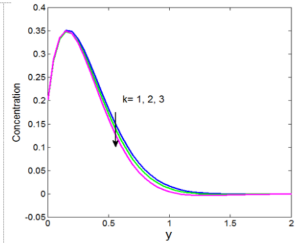

Figure 13: Species concentration profiles for various values of *k* when R=1

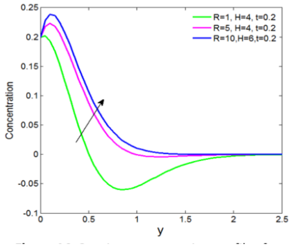

Figure 14: Species concentration profiles for various values of *R* and *H*

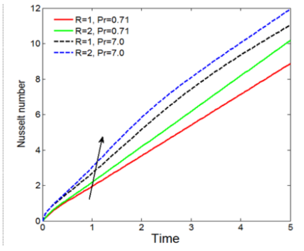

Figure 15: Nusselt number for various values of Pr and *R*

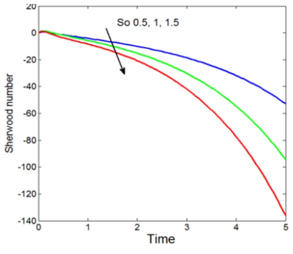

Figure 16: Sherwood number for various values of *So*

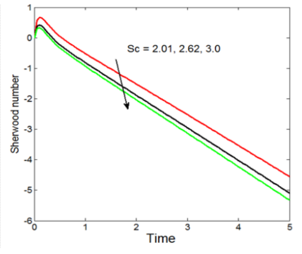

Figure 17: Sherwood number for various values of *Sc*

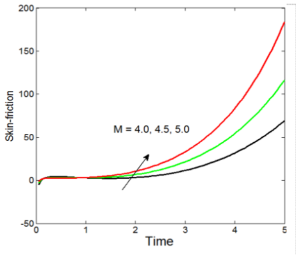

Figure 18: Skin-friction for various values of *M*

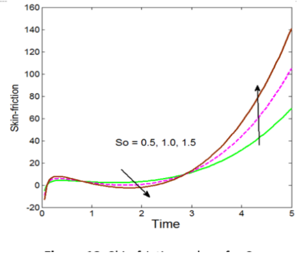

Figure 19: Skin friction values for So

CONCLUSIONS:

The intention of this study was to get exact solutions for the effects on unsteady MHD Casson fluid due heat and mass transfer. Under the influence of uniform transverse magnetic field, fluid past a vertical plate when Porous Medium is present with variable concentration and variable temperature. With the help of Laplace transform technique the expressions for the temperature, the velocity, and concentration have been derived in closed form. The effects of the appropriate parameters on velocity, temperature and concentration profiles are showed in form of graphs. The conclusions of the study are as follows:

- The velocity decreases with an increase in magnetic parameter.
- The velocity increases with an increase in Casson parameter.
- The velocity increases with increasing of Soret number.
- The temperature decreases with increasing *R* or *H* or *t*.
- The temperature decreases with increasing Prandtl number.
- Nusselt number increases with increasing *R* or *Pr*.
- Sherwood number decreases with increasing of *So*
- Skin-friction increases with increasing of magnetic parameter.

REFERENCES:

[1] Alam Md S, Rahman Md M. Dufour and Soret effects on MHD free convective heat and mass transfer flow past a vertical porous flat plate embedded in a porous medium. Journal of Naval Architecture and Marine Engineering 2009; 2(1):55-65. http://dx.doi.org/10.3329/jname.v2i1.2030

[2] Ahmmed, S. F., Analytical Study on Unsteady MHD Free Convection and Mass Transfer Flow Past a Vertical Porous Plate. American Journal of Applied Mathematics 3 (2), 64, 2013. http://dx.doi.org/10.11648/j.ajam.20150302.16

[3] Animasaun, I.L. "Effects of thermophoresis, variable viscosity and thermal conductivity on free convective heat and mass transfer of non-Darcian MHD dissipative Casson fluid flow with suction and nth order of chemical reaction", Journal of the Nigerian Mathematical Society 34 (2015) 11–31. http://dx.doi.org/10.1016/j.jnnms.2014.10.008

[4] Chamaka A.J, and Abdul-Rahim A. Khaled, "Hydro magnetic combined heat and mass transfer by natural convection from a permeable surface embedded in a fluid saturated porous medium", Int. Journ. Num.Methods for Heat and Fluid flow, 2000, 10(5), 455-476. http://dx.doi.org/10.1108/09615530010338097

[5] Cogly A.C, Vincenti W.G, and Gill S.E, "Differential Approximation for Radiative Transfer in a non gray gas near equilibrium", AIAA J.,1968, Vol.6, 551-553. http://dx.doi.org/10.2514/3.4538

[6] Cramer K.P, and Pai S.I, "Magneto fluid dynamics for Engineers and Applied Physics", New York,1973, McGraw-Hill Book Co.

[7] Das, U. N., Deka, R.K., and Soundalgekar, V.M.: Radiation effects on flow past an impulsively started vertical infinite plate, J.theo. Mech. 1(1996), 111-115. http://dx.doi.org/10.1007/bf02601318

[8] Emmanuel Maurice Arthur, Ibrahim Yakubu Seini, Letis Bortey Bortteir, Analysis of Casson Fluid Flow over a Vertical Porous Surface with Chemical Reaction in the Presence of Magnetic Field. Journal of Applied Mathematics and Physics 03 (06), 713 to 723, 2015. http://dx.doi.org/10.4236/jamp.2015.36085

[9] Gebhart, B., and Pera, L.: Heat Mass Transfer.Int.J.14 (1971), 957.2.http://dx.doi.org/10.1016/0017-9310(71)90123-2

[10] Hari R. Kataria, Harshad R. Patel., Radiation and chemical reaction effects on MHD Casson fluid flow past an oscillating vertical plate embedded in porous medium. Alexandria Engineering Journal vol 55 (1), 583 -595, 2016. http://dx.doi.org/10.1016/j.aej. 2016.01.019

[11] Hayat T, Mustafa M, and Pop I,"Heat and mass transfer for Soret and Dufour's effect on mixed convection boundary layer flow over a stretching vertical surface in a porous medium filled with a viscoelastic fluid," Commn. Nonl. Sci. and Numeric.Simul., 2010, vol. 15 (5), 1183–1196. http://dx.doi.org/10.1016/j.cnsns.2009.05.062

[12] Hayat, T., Shehzad, S.A., Alsaedi, A. and Alhothuali, M.S. (2012) Mixed Convection Stagnation Point Flow of Casson Fluid with Convective Boundary Conditions. Chinese Physics Letters, 29, Article ID: 114704. http://dx.doi.org/10.1088/0256-307X/29/11/114704

[13] Hossain M.A, Alim M.A, and Rees D.A.S,"The effect of radiation on free convection from a porous vertical plate", Int. J. Heat Mass Transfer, 42, 1999, 181 - 191. http://dx.doi.org/10.1016/s0017-9310(98)00097-0

[14] Khalid, A., Khan, I., Arshad Khan, and Sharidan Shafie, Unsteady MHD free convection flow of Casson fluid past over an oscillating vertical plate embedded in a porous medium. Engineering Science and Technology, an International Journal vol 18 (3), 309 to 317, 2015. http://dx.doi.org/10.1016/j.jestch.2014.12.006

[15] Mabood, F., Khan, W.A. and Ismail. A.I.M. Multiple slips effects on MHD Casson fluid flow in porous medium with radiation and chemical reaction, Canadian Journal of Physics 94 (1), 26-34, 2016. http://dx.doi.org/10.1139/cjp-2014-0667

[16] Makinde OD. On MHD boundary-layer flow and mass transfer past a vertical plate in a porous medium with constant heat flux International. Journal of Numerical Methods for Heat and Fluid Flow 2009; 19(3/4): 546-554.http://dx.doi.org/10.1108/ 0961553091 09 38434

[17] Makinde, O.D & Aziz, A, "MHD-mixed convection from a vertical plate embedded in a porous medium with a convective boundary condition", Int.Journ. Thermal Sciences,2010,49, 1813-1820. http://dx.doi.org/10.1016/j.ijthermalsci.2010.05.015

[18] Mustafa, M., Hayat, T., Pop, I. and Hendi, A. A., Stagnation-point flow and heat transfer of a Casson fluid towards a stretching sheet. Z. Naturforsch., 67a, p.70 (2012).

[19] Muthucumaraswamy, R., and Janakiraman, B.: MHD and radiation effects on moving isothermal vertical plate with variable and mass diffusion, Theo. Appl. Mech. 33(1) (2006), 17-29. http://dx.doi.org/10.2298/tam0601017m

[20] Pramanik, S., Casson fluid flow and heat transfer past an exponentially porous stretching surface in presence of thermal radiation. Ain Shams Engineering Journal volume 5 issue 1 on pp 205 to 212, 2014.http://dx.doi.org/10.1016/j.asej.2013.05.003

[21] Rushi Kumar B, Gangadhar K. Heat generation effects on MHD boundary layer flow of a moving vertical plate with suction, Journal of Naval Architecture and Marine Engineering 2012; 9 (2):153-162. http://dx.doi.org/10.3329/janme.v9i2.8550

[22] Rushi Kumar B, Sravan Kumar T, Vijaya Kumar AG. Thermal Diffusion and Radiation Effects on Unsteady Free Convection Flow in the Presence of Magnetic Field Fixed Relative to the Fluid or to the Plate. J. Frontiers in Heat and Mass Transfer 2015; 6:6-12. http://dx.doi.org/10.5098/hmt.6.12

[23] Shehzad, S. A., Hayat, T., Qasim, M. and Asghar, S., Effects of mass transfer on MHD flow of casson fluid with chemical reaction and suction. Brazilian Journal of Chemical Engineering volume 30 issue 1 on pages 187 to 195, 2013 http://dx.doi.org/10.1590/s 0104- 66322013000100020

[24] Soundalgekar, V.M., Patil, M.R., and Jahagirdar, M.D. MHD Stokes problem for a vertical plate with variable temperature, Nuclear Eng. Des. 64(1981), 39-42. http://dx.doi.org/10.1016/0029-5493(81)90030-3

[25] Swati Mukhopadhyay. Casson fluid flow and heat transfer over a nonlinearly stretching surface. Chinese Physics B volume 22 issue 7 on page 074701, 2013. http://dx.doi.org/10.1088/1674-1056/22/7/074701

[26] Tokis, J.N.: A class of exact solutions of the unsteady magneto hydrodynamic free-convection flows, Astrophysics. Space Sci. 112, 413–422 (1985). http://dx.doi.org/ 10. 1007/ bf00653524